SUPPORTING MATERIAL

Quantification of Biomass and Cell Motion in Human Pluripotent Stem Cell Colonies

Thomas A. Zangle, Jennifer Chun, Jin Zhang, Jason Reed, and Michael A. Teitell

Supporting Movies S1-S4:
Movies illustrating colony motion and LCI time-lapse measurements of mass distributions. Movies S1 and S2 each show one untreated (control) colony for 110 and 45 minutes, respectively. Movie S3 shows a colony from day 4 of retinoic acid treatment over a period of 80 minutes. Movie S4 shows a colony from day 6 retinoic acid treatment over a period of 50 minutes.

Supporting Figures S1-S7:
Fig. S1: LCI mass measurements for colonies of identical area.
Fig. S2: Immunofluorescence, embryoid body, and *OCT4* mRNA expression for pluripotency characterization.
Fig. S3: Lognormal fits, summary of growth rate statistics, cell counting data, and effect of colony size on mass accumulation rate and power law fit.
Fig. S4: Additional gene expression and cell cycle data.
Fig. S5: Phase and fluorescence measurements illustrating single cell mass measurement for a sample colony.
Fig. S6: Calibration measurements of polystyrene beads showing insensitivity of LCI measurements to cell morphology.
Fig. S7: Additional local mass accumulation/depletion plots.
Fig. S8: Supporting data for Fig. 7.

Supporting Analysis: Theoretical growth rate versus mass for large colonies

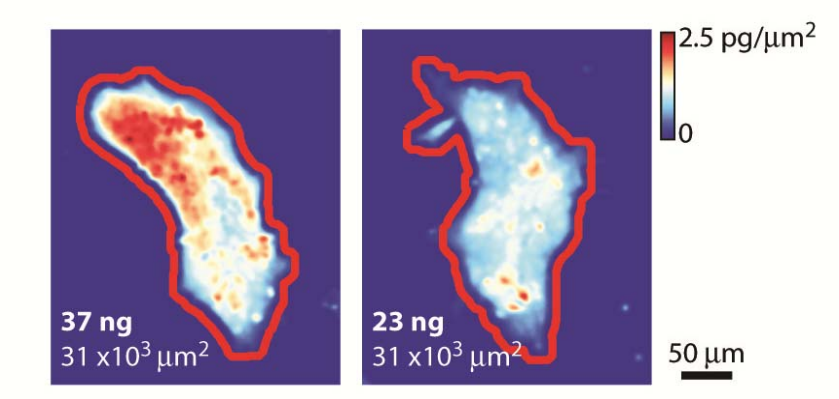

FIGURE S1. The LCI can determine mass differences in transparent objects of identical area, demonstrating the need for quantitative mass measurements to determine accurate sizes for hPSC colonies. Red outline shows the automatically detected border for these two HSF1 colonies of identical area but unequal mass. In all hPSC measurements, mass is quantified by adding the mass at each imaging pixel within red borders.

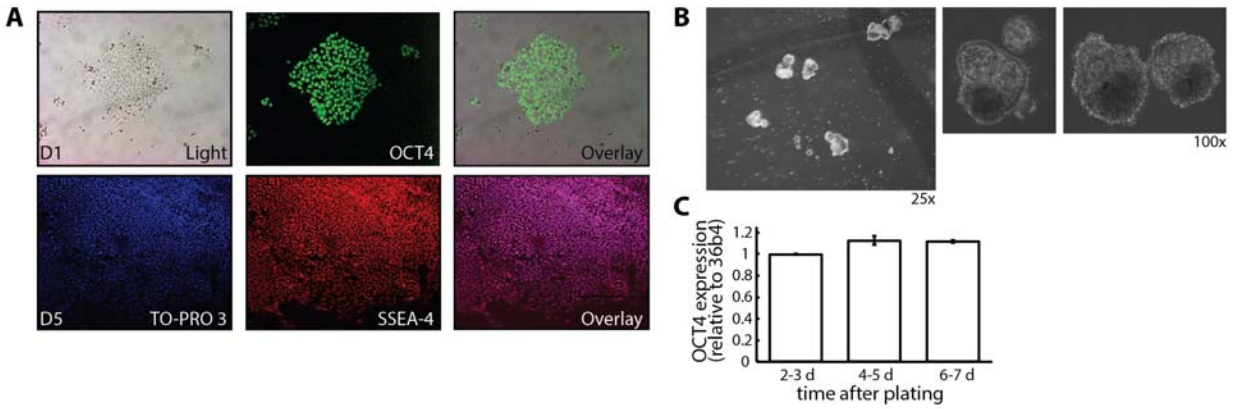

FIGURE S2. (*A*) Colony morphology of hESCs (HSF1) grown on MEF feeder free Matrigel plate. OCT4 and SSEA-4 staining with immunofluorescence indicates their pluripotency. TO-PRO3 is a nuclear stain to show colocalization of SSEA-4 staining. (*B*) Embyoid bodies formed from hESC line HSF1 used in this study. The three-dimensional spheroid aggregates of differentiated pluripotent cells were cultured in EB media for ~10 d, and resembled early embryonic germ-layer development. The outer layer of cells represent differentiated trophoectoderm and the darker region in the embryoid body represent formation of embryonic cavity. EBs have the potential to differentiate into three, typically disorganized, germ layers. (*C*) *OCT4* gene expression data over 6-7 days in culture shows maintenance of pluripotency. Error bars show SE.

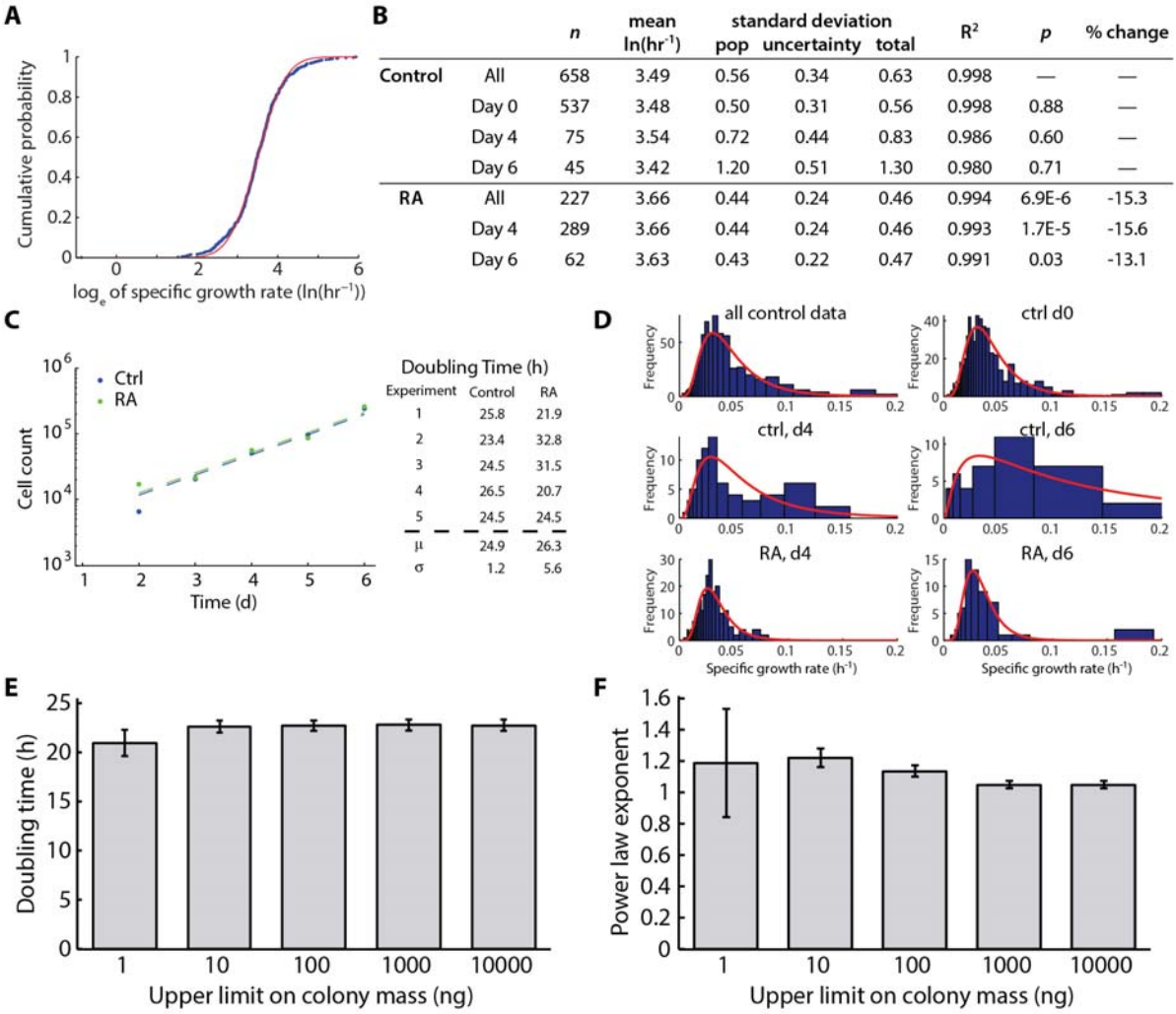

		n	mean ln(hr^{-1})	standard deviation pop	uncertainty	total	R^2	p	% change
Control	All	658	3.49	0.56	0.34	0.63	0.998	—	—
	Day 0	537	3.48	0.50	0.31	0.56	0.998	0.88	—
	Day 4	75	3.54	0.72	0.44	0.83	0.986	0.60	—
	Day 6	45	3.42	1.20	0.51	1.30	0.980	0.71	—
RA	All	227	3.66	0.44	0.24	0.46	0.994	6.9E-6	-15.3
	Day 4	289	3.66	0.44	0.24	0.46	0.993	1.7E-5	-15.6
	Day 6	62	3.63	0.43	0.22	0.47	0.991	0.03	-13.1

FIGURE S3. (*A*) Gaussian cumulative density function (cdf) fit, in red, to the empirical cumulative probability, in blue, demonstrating the method used to estimate the mean and standard deviation of specific growth rate. Data shown is for all control colonies. (*B*) Summary of results for cdf fitting and Monte Carlo routine incorporating uncertainty in measured colony growth rates. *n* is number of colonies in each category. Mean and standard deviation are presented as the mean of the logarithm base *e* of the specific growth rate (hr^{-1}). Standard deviations are presented for: the population without uncertainty, the distribution of means due to consideration of uncertainty in growth rate (this is the standard deviation of all sample means from the Monte Carlo analysis), the total standard deviation (due to both underlying population standard deviation and uncertainty in growth rate, calculated as the average standard deviation from all cdf curve fits in the Monte Carlo analysis). R^2 quantifies goodness of fit for the cdf fit to the population data (as in *A*). *p* values and percent change are calculated relative to all control data. (*C*) Sample cell counting data used to estimate proliferation rate with linear best fit line (on logarithmic scale) used to calculate doubling rate and all doubling times as determined in each cell counting experiment. (*D*) Lognormal curve fits for individual measurement days, as in Figure 3*B*. (*E, F*) Performing the specific growth rate analysis (*E*) or power law scaling analysis (*F*) for restricted ranges of colony size has little effect on the final result. Error bars show s.d.

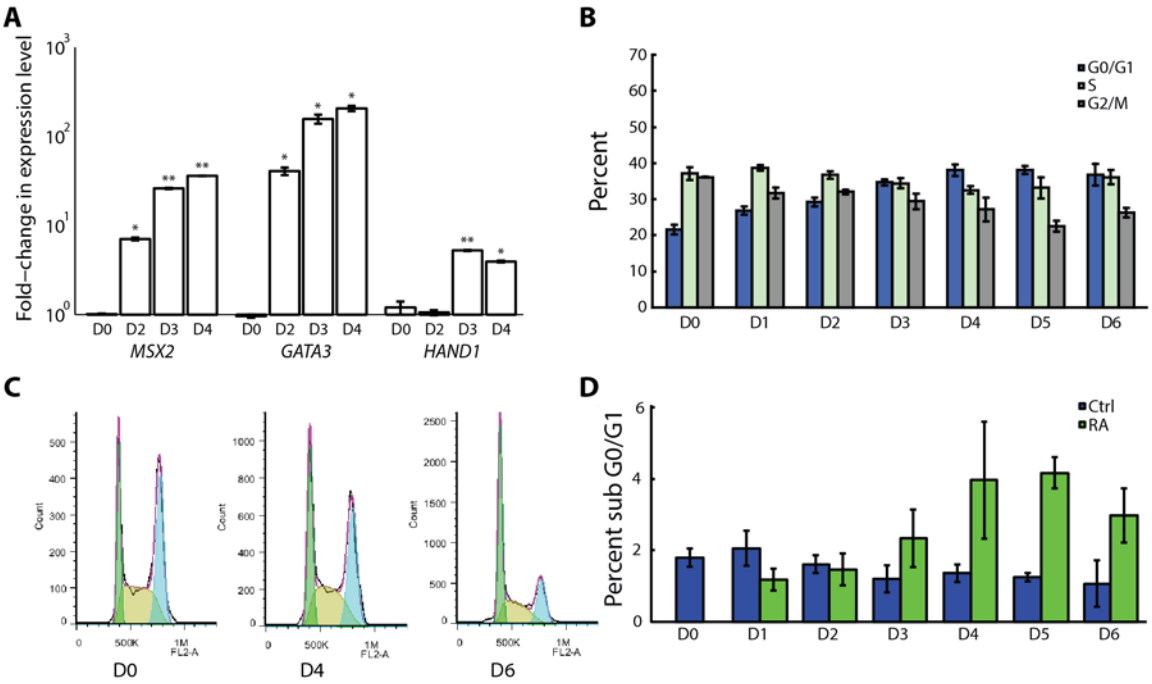

FIGURE S4. (*A*) changes in hPSC expression of *MSX2*, *GATA3* and *HAND1* trilineage differentiation genes after 0, 2, 3 and 4 d of RA exposure. (*B*) Cell cycle analysis of cells from control colonies on successive days of the experiment. (*C*) Representative YOYO-1 fluorescence intensity curve fits for RA-treated cells at 0, 4 and 6 d. (*D*) Percent sub-G0/G1 cells over 6 days of RA treatment. Error bars show SE, *$p<0.05$, **$p<0.01$ relative to control data.

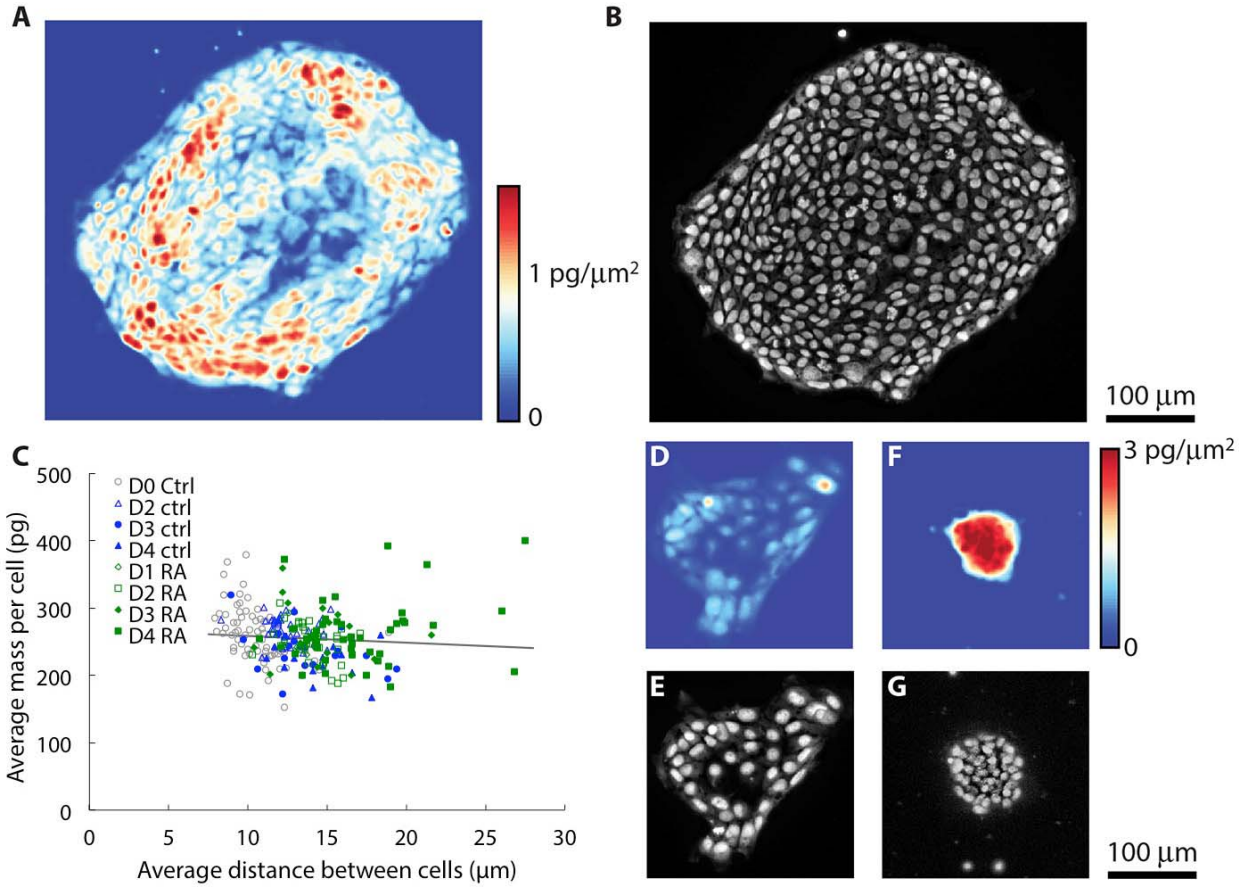

FIGURE S5. Phase and fluorescence measurements illustrating single cell mass measurement for sample colonies and average mass per cell as a function of the distance between cells. (*A*) Quantitative phase image of a colony from d 4 of RA treatment with a total mass of 90.6 ng. (*B*) The corresponding fluorescence image of YOYO-1 stained nuclei gives a count of 392 cells. Together this yields 231 pg as the estimated average mass per cell. (*C*) Average mass per cell plotted against the average distance between cells with least squares best fit line shown in dark grey. The average distance between cells increases as colonies take on a more differentiated appearance. The slope of this line is not statistically significant from zero, indicating that there is no evidence for a relationship between these two parameters, further supporting the conclusion that cell mass is unchanged during early differentiation. (*D*, *E*) Phase and fluorescence images of sample RA-treated colony (day 4 of treatment) with an average distance between cells of 19.9 μm and an average mass per cell of 277 pg. (*F*, *G*) Phase and fluorescence images of sample control, untreated colony (24 hours after plating) with an average distance between cells of 10.1 μm and an average mass per cell of 232 pg.

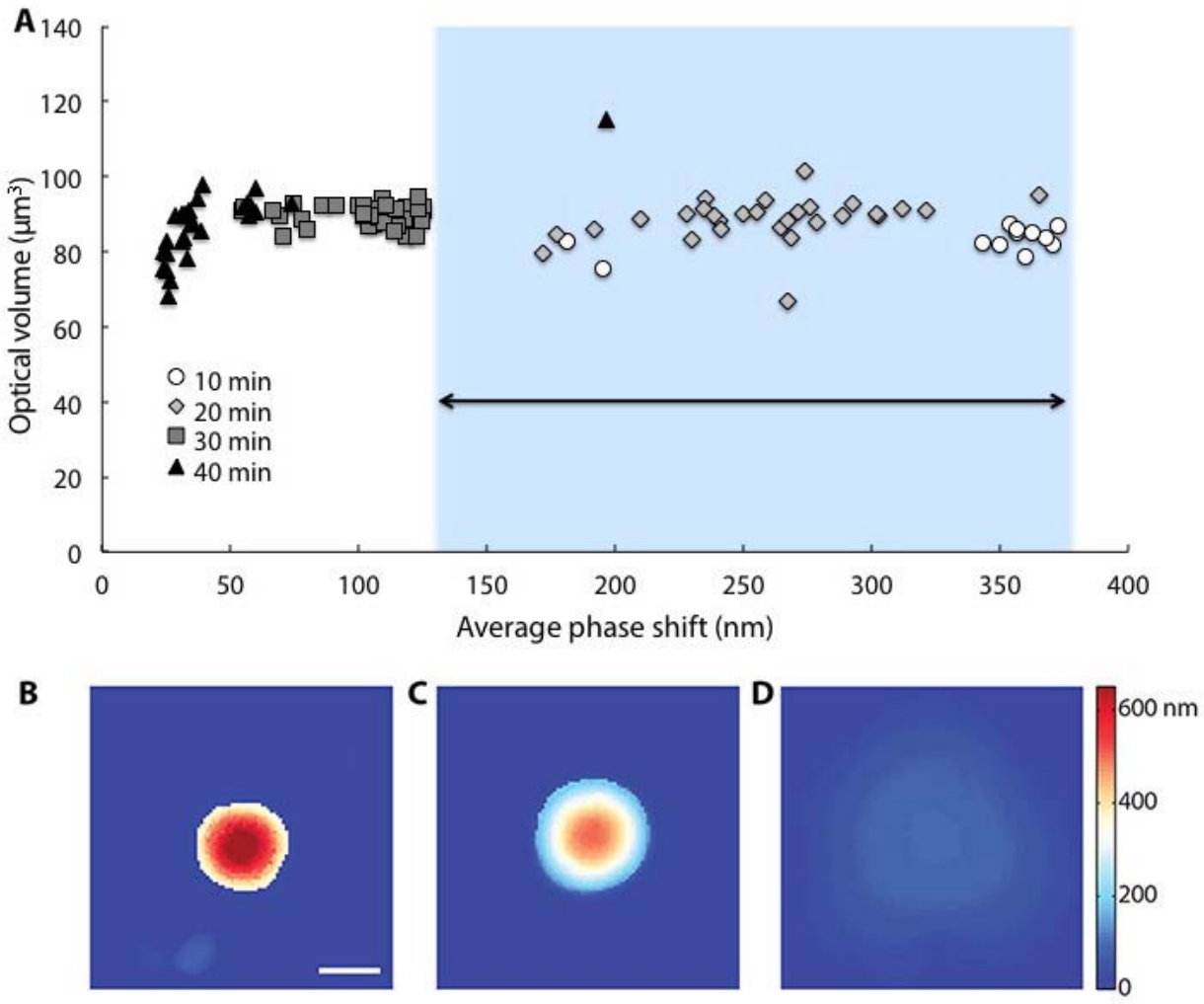

FIGURE S6. Calibration measurements of polystyrene beads melted onto a silicon substrate for the indicated amount of time to generate calibration standards of uniform optical volume, with variable average phase shift from very flat beads (low average phase shift) to very high, round beads (high phase shift). (*A*) Typical stem cell colony measurement range indicated in blue, showing that LCI measurements of stem cell mass are insensitive to changes in cell morphology shift over the range of measured phase shifts. (*B*)-(*D*) images of polystyrene beads melted for 10 (*B*), 20 (*C*), and 40 (*D*) minutes with average phase shifts of 372, 240, and 60 nm, respectively. These melted beads all have measured optical volumes equal to the overall mean +/- 2.6%. Scale bar in (*B*) is 10 μm.

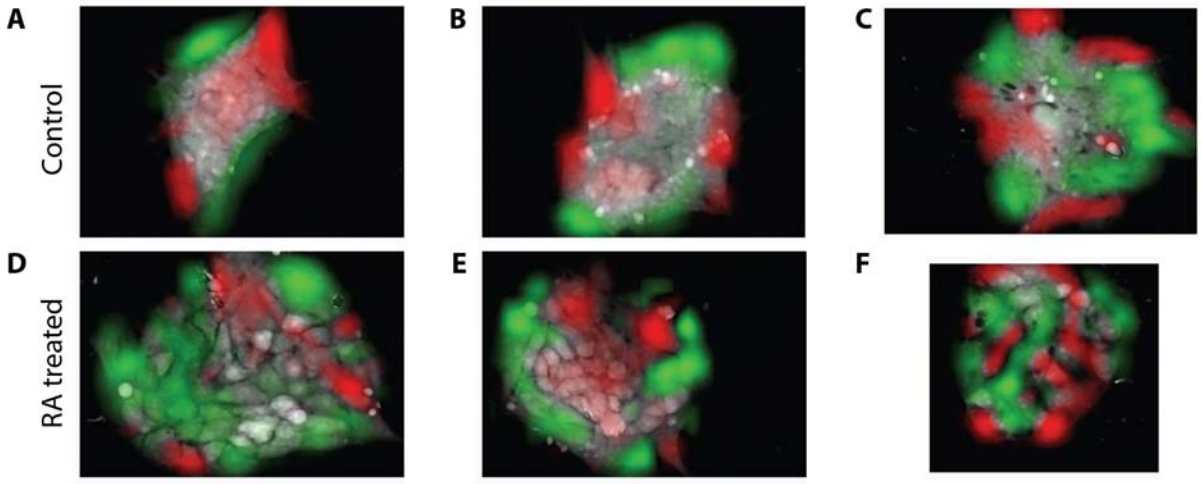

FIGURE S7. Additional local mass accumulation plots, as in Figure 6*A* and *D*. Top row shows control colonies. Bottom row shows RA-treated colonies.

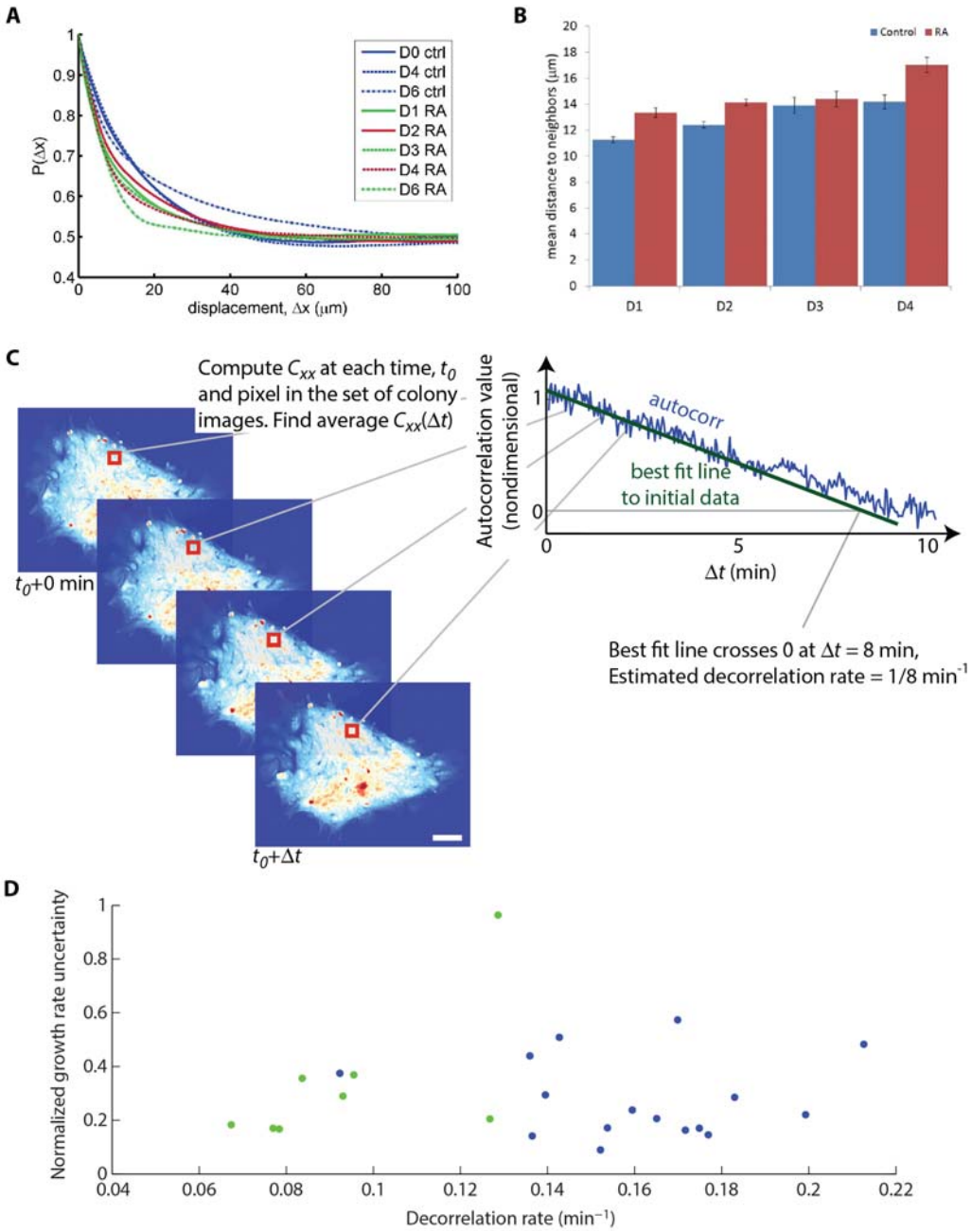

FIGURE S8. (*A*) $P(\Delta x)$ vs. displacement for all RA colonies, including those measured after 1-3 d of RA treatment showing the gradual loss of coordination during the first two days of RA treatment. n = 62, 121 and 106 for 1, 2 and 3 d of RA treatment. (*B*) Average distance between cells for control and RA-treated colonies, based on distance between nuclei centers from fluorescence images. (C) Illustration of decorrelation timescale. Average autocorrelation, C_{xx}, is computed across all pixel locations within the image stack. Then a linear best fit line is applied to the initial 5 minutes of $C_{xx}(\Delta t)$. Δt at the zero crossing of this line defines the decorrelation timescale. The inverse of this timescale is the decorrelation rate. Error bars show SE. (*D*) normalized uncertainty in growth rate measurement (calculated as the standard deviation of the growth rate estimate) plotted against the decorrelation rate. Intracolony motion shows no effect on the uncertainty in growth rate.

Supporting Analysis: Theoretical growth rate vs. mass for large colonies

In this section we will show that the observed linear relationship between colony mass accumulation and growth rate is expected regardless of the mass vs. time relationship of individual cells within the colony, assuming a constant average cell mass and interdivision time. Our results indicate that the average growth rate per mass (biosynthetic capacity) stays constant as colony size increases (Fig. 3 *A*) and we see no evidence for a change in average cell size with increasing colony size (Fig. 5 *A*). Given a constant average cell mass, interdivision time (which is the average time for a cell to double its mass) should remain linked to average cell mass accumulation rate. A significant, transient divergence in these two rates (growth and proliferation) would occur if there were a change in the average cell size. For example, if cell average mass were to increase significantly, at constant mass accumulation rate, we would expect a transient delay in cell proliferation rate, until the population re-established itself at the new average mass. However, in light of the observation of nearly constant cell mass with increasing colony size, in the present case, interdivision time should remain linked to the average cell mass accumulation rate, and the assumption of constant interdivision time with increasing colony size should hold.

We start by considering the total mass, M, of a colony composed of n individual cells, m_i, given by:

$$M = \sum_{i=1}^{n} m_i \, .$$

First, we will look at the relationship between the mass accumulation rate of the colony and the masses of the individual cells which comprise that colony. Differentiation in time yields the rate of mass accumulation of the colony in terms of the mass accumulation rate of each of its constituent cells:

$$\frac{dM}{dt} = \sum_{i=1}^{n} \frac{dm_i}{dt} \, .$$

If we assume that n is large, and that the cells in the colony are not cell-cycle synchronized (which is consistent with our observation that only a small, consistent fraction of cells within large colonies stained for DNA are mitotic), then we can write:

$$\frac{dM}{dt} \approx n\overline{\frac{dm}{dt}} \, ,$$

where $\overline{dm/dt}$ is the average mass accumulation rate of an individual cell across the cell cycle. If we assume that each individual cell starts at an initial mass, m_0, and divides when it reaches twice this size, then we can write:

$$\overline{\frac{dm}{dt}} = \frac{1}{t_{cycle}} \int_0^{t_{cycle}} \frac{dm}{dt}(t)\, dt = \left[m \right]_0^{t_{cycle}} = \frac{m_0}{t_{cycle}} \, .$$

Therefore:

$$\frac{dM}{dt} = n\frac{m_0}{t_{cycle}} \, .$$

Now we will consider the relationship of the colony total mass to the mass of its constituent cells. Given the same assumptions above, for the total mass of the colony, we can write:

$$M \approx n \cdot \overline{m} \, ,$$

where $\overline{m}$ is the cell-cycle averaged mass of the cells within the colony:

$$\overline{m} = \frac{1}{t_{cycle}} \int_0^{t_{cycle}} m(t)\, dt \,.$$

Before we consider the general case, first, consider the case of purely exponential mass accumulation, $m = m_0 e^{t/\tau}$, where m is the mass of an individual cell, m_0 is the mass of this cell at division, t is time, and τ is the exponential time constant for mass accumulation ($\tau \ln(2) = t_d$, where t_d is the doubling time for mass). In this case:

$$\overline{m} = \frac{m_0}{t_{cycle}} \tau \left(e^{t_{cycle}/\tau} - 1 \right).$$

Recognizing that $2m_0 = m_0 e^{t_{cycle}/\tau}$:

$$\overline{m} = \frac{m_0}{t_{cycle}} \tau \,.$$

Plugging this into our relationship for total colony mass, and combining with the relationship for colony average mass yields:

$$M = n \frac{m_0}{t_{cycle}} \tau = \tau \frac{dM}{dt} \,.$$

Therefore, if the cell cycle parameters stay constant with increasing colony size, the expected colony mass accumulation rate is directly proportional to the total mass of the colony.

Next, if we consider the general case where m is continuous and lies on the interval $[m_0, 2m_0]$ over the duration of a cell cycle of duration t_{cycle}, with $t \in [0, t_{cycle}]$, by the mean value theorem we can write:

$$\overline{m} = \frac{1}{t_{cycle}} \int_0^{t_{cycle}} m(t)\, dt = \frac{m(c)}{t_{cycle}},$$

where $c \in [0, t_{cycle}]$, therefore the average mass, $\overline{m}$, is equal to some value on the interval $[m_0, 2m_0]$. This means, for any mass vs. time relationship, we can find a number, k, such that:

$$\overline{m} = k \cdot \frac{m_0}{t_{cycle}} \,.$$

Therefore, we can write:

$$M = n \cdot k \cdot \frac{m_0}{t_{cycle}} = k \frac{dM}{dt} \,.$$

Again, the colony mass accumulation rate is directly, linearly proportional to the total mass of the colony, as long as the parameter k is independent of colony size. If k were dependent on colony size, we would expect a the relationship between M and dM/dt to be described by a super- or sub-linear, powerlaw relationship. Therefore, to test this model prediction, we perform nonlinear least squares fitting to a powerlaw, $M = k(dM/dt)^p$, where p is the scaling exponent. Also, note that the constant of proportionality, k, can be easily computed for any other assumed

mass accumulation profile. For example, in the exponential case above, $k = \tau$, or in the case of constant, linear growth, $m = m_0\left(t / t_{cycle} + 1\right)$, $k = \frac{3}{2} t_{cycle}$.